JOURNAL OF APPLIED ELECTROCHEMISTRY 21 (1991) 446–451

The influence of the electrochemical treatment on Cu–Al–Ag alloys in deaerated 0.5 M NaOH

P. L. CABOT*, F. A. CENTELLAS, J. A. GARRIDO

Dep. de Química Física, Facultat de Química, Universitat de Barcelona, Avda. Diagonal, 647, 08028-Barcelona, Spain

P. T. A. SUMODJO

Dep. de Química Fundamental, Inst. de Química, Universidade de São Paulo, C.P. 20780, 01498-São Paulo, S.P., Brazil

A. V. BENEDETTI, R. Z. NAKAZATO

Dep. de Físico-Química, Inst. de Química, Universidade Estadual Paulista, C.P. 355, 14800-Araraquara, S.P., Brazil

Received 21 February 1990; revised 10 October 1990

The effect of consecutive cyclic polarization in de-aerated 0.5 M NaOH solutions on the surface microstructure of mechanically polished Cu–Al–Ag alloys of different compositions and heat treatments has been studied using optical microscopy, SEM and EDS. The current peaks of the cyclic polarization curves do not depend on the alloy composition in the composition range studied. The repetitive potential scans between H_2 and O_2 evolution in alkaline media lead to preferential dissolution of aluminium, the roughness and phase composition of the surface of the alloys changing significantly. The quasistationary *I–E* curves of the different Cu–Al–Ag alloys studied consist in the superposition of the quasistationary *I–E* curves of high-purity Cu and Ag, the EDS microanalysis showing that aluminium is not present on the surface of the alloy in these conditions.

1. Introduction

The many technological applications of copper have led to the development of several Cu based alloys. The Cu–Al–Ag alloys are regarded as interesting new materials, due to their good mechanical properties, such as high plasticity and workability, and to their high corrosion resistance in different media [1–5]. Certain Cu–Al–Ag alloys are of interest in electronics and odontology.

Several of these copper based alloys have been studied from the viewpoints of metallography, mechanical properties and activation energy of the precipitate growth process (silver enriched phase) [1–4, 6, 7]. However, little attention has been devoted to their electrochemical behaviour in different electrolytes. Recent studies in our laboratories have shown that the alloy Cu(89.4%)–Al(5.4%)–Ag(5.2%) has a very low corrosion rate in artificial saliva [5] and it is of interest to obtain a better understanding of the electrochemical stability of the copper based alloys in different conditions. Preliminary potentiodynamic results on the extruded Cu(79.5%)–Al(10.5%)–Ag(10.0%) alloy in de-aerated 0.5 M NaOH at 30° C were examined [8]. In such a preliminary communication, the quasistationary *I–E* curves between H_2 and O_2 evolution were obtained and the peaks assigned by comparing such curves with those corresponding to the pure metals. Any influence of aluminium in the quasistationary *I–E* curves was not detected.

Potential perturbation programmes, when applied to solid electrodes, are able to cause structural and morphological modifications on their surfaces and, therefore, changes in crystallographic orientation and composition are possible to successive electrochemical oxidations and reductions. In the present paper, the objective is to examine the microstructural features of three Cu–Al–Ag alloys of different compositions when subjected to an electrochemical perturbation programme in 0.5 M NaOH. Such results are necessary to the interpretation of the polarization behaviour planned in further work.

The surface of the alloys was examined by means of metallographic and scanning electron microscopy, the surface microanalysis performed by EDS and, when required, the concentration of the species dissolved in the working electrode after the electrochemical treatment were determined.

2. Experimental details

The alloys studied in this work were prepared from

* Author to whom correspondence should be addressed.

0021-891X/91 $03.00 + .12

Table 1. Chemical composition of the alloys, % in weight, determined by spectrographic analysis

Alloy	*Cu*	*Ag*	*Al*	*Fe*	*Si*	*Pb*	*Zn*	*Mg*
A	81.83	9.95	8.08	0.12	0.01	–	0.01	0.005
B	73.35	18.60	7.60	0.18	0.01	0.25	0.01	0.005
C	61.53	30.00	8.30	0.15	0.01	–	0.01	0.005

99.99% Cu, Al and Ag according to the procedure described elsewhere [6]. Table 1 lists the alloy compositions determined by spectrographic analysis. Alloy A was only extruded, while alloys B and C were also annealed for 400 hours to obtain the equilibrium structure at 25° C.

All the electrochemical studies were performed in a conventional three electrode cell. The working electrodes were made by encapsulating alloy cylinders in epoxy resin, exposing to the solution a disc with diameter ranging from 0.25 to 0.40 cm. The counter electrode was a large area platinized Pt wire. Electrode potentials were measured with respect to a reversible hydrogen electrode in the same solution (HESS). All the potentials given in this work are referred to this electrode. All the experiments were carried out with 50 cm^3 of de-aerated 0.5 M NaOH at 25° C. The working solutions were prepared from Merck p.a. NaOH and Milli-Q quality water. Before each experiment, the specimen was mechanically polished with emery paper of different grades.

The electrochemical perturbation programme applied to the electrodes consisted of a repetitive triangular potential sweep (RTPS) at 100 mV s^{-1}, between H_2 and O_2 evolution, i.e. between −0.50 and +1.70 V. Although the sweep rate was constant for each RTPS, the effect of the sweep rate on the quasistationary cyclic polarization curve was also examined. Preliminary experiments demonstrated that peak currents and potentials changed gradually with the number of consecutive polarization cycles. In order to analyse the effect of the cyclic potential scan on the surface of the alloys, such cyclic polarization was always stopped at −0.50 V. Immediately after the electrochemical perturbation, the electrode was rinsed with Milli-Q water, dried in N_2 atmosphere and stored under high vacuum. The working solutions were analysed after the RTPS by means of a JOBIN YVON JY38VHR inductively coupled argon plasma spectroscope.

The specimens were examined in a Carl-Zeiss METAVAL metallographic microscope and in a JEOL-JSM 840 SEM. The surface microanalysis was performed by energy-dispersive X-ray spectroscopy (EDS). From the microscope operation voltage and the mean density of the material, the electron penetration depth was estimated to be between 0.45 and 0.55 μm. In order to perform the metallographic examinations, some polished cross-sections were etched in the reagents: R_1, composed of 50 cm^3 of HNO_3 (60% w/w), 20 g of Cr_2O_3 and 30 cm^3 of H_2O and R_2, composed of 30 cm^3 of HCl (37% w/w), 5 g of $FeCl_3$, 30 cm^3 of isoamyl alcohol, 30 cm^3 of ethyl alcohol and 5 cm^3 of H_2O.

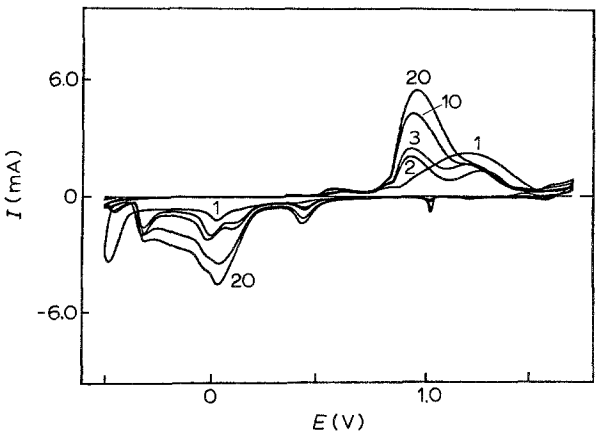

Fig. 1. First consecutive cyclic polarization curves of alloy A at 100 mV s^{-1} between H_2 and O_2 evolution. The number of the cycles performed are indicated on the corresponding curve.

3. Results and discussion

When the Cu–Al–Ag alloys are submitted to consecutive cyclic polarization between H_2 and O_2 evolution, that is between −0.50 and +1.70 V with respect to HESS, respectively, the corresponding *I–E* curves change gradually as indicated in Fig. 1. The form of these curves does not depend on the alloy composition in the range of compositions studied. The first cycles show the major differences in peak currents and potentials. However, after about 10 consecutive cycles, only slight differences in peak currents and potentials are found. At sweep rates between 25 and 100 mV s^{-1}, the quasistationary *I–E* curves are

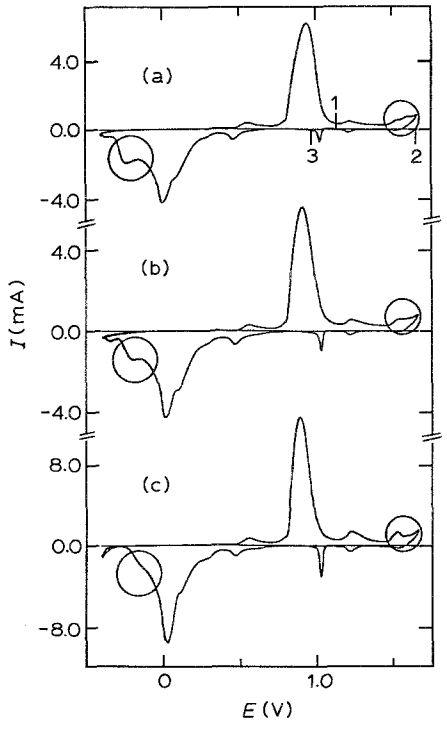

Fig. 2. Quasistationary cyclic polarization curves after 1 h of RTPS at 25 mV s^{-1}: (a) alloy A (cross-section of 0.049 cm^2); (b) alloy B (cross-section of 0.053 cm^2) and (c) alloy C (cross-section of 0.120 cm^2).

obtained after about 1 h of RTPS. When the sweep rate decreases, the differences in the first consecutive cyclic polarizations and the quasistationary curve are not so great.

The quasistationary *I–E* curves at 25 mV s^{-1} for the three Cu–Al–Ag alloys studied are shown in Fig. 2. As expected, the curve corresponding to the alloy A, i.e. Fig. 2a, has the same current peaks as the quasistationary *I–E* curve at 100 mV s^{-1} for the extruded alloy of very similar composition previously studied (10.5% in Al and 10.0% in Ag) [8]. As shown in Figs 2b and 2c, the quasistationary *I–E* curves corresponding to the annealed alloys, i.e., alloys B and C, show only minor differences in the form of the peaks and the peak potentials when compared with Fig. 2a. As found with the Cu–Al–Ag alloy previously studied, the current peaks shown in Figs 2a–2c correspond to the superposition of the quasistationary *I–E* curves of high-purity copper and silver and, therefore, the same peak assignation can be adopted: silver is oxidized at potentials more anodic than point 1 (Fig. 2a); between points 1 and 2, copper and silver are both oxidized; in the cathodic sweep, silver oxidized species are reduced between points 2 and 3, while copper oxidized species are reduced at potentials more negative than point 3. The voltammograms shown in Fig. 2 only exhibit a few differences which are circled in the figure. It is observed that the current peak associated with the oxidation of interphase species Ag(I) to Ag(II), at ~ 1.625 V, appears as a doublet when the silver content in the alloy is diminished. This can be explained by the fact that in this potential region, copper and silver are both electroactive and the doublet is noted just for the highest concentration of copper studied. For higher concentrations of silver, the peak corresponding to the latter metal increases and does not permit observation of the copper peak. The other difference corresponds to the reduction of copper surface species, at ~ -0.125 V. Silver is not electroactive in the latter potential region and, therefore, the multiplicity of the copper peak ~ -0.125 V is probably attributable to the reduction of different species or the same species on different crystallographic sites.

Quasistationary cycles in Fig. 2 show differences in peak currents due, on one hand, to the different cross-sections of the alloys and, on the other hand, to the different copper and silver contents. When considering the cross-sections of the alloys studied, the peak currents of copper species shown in Fig. 2 are proportional to the copper content of the alloy and the peak currents corresponding to silver species are proportional to the silver content.

In order to understand the changes caused by the RTPS on the surface of the alloy, surface characterization was performed by means of metallographic assays, SEM and EDS, before and after the RTPS. Metallographic microscopic examination reveals that the surface of the annealed alloys, that is samples B and C, exhibit three different regions, the grain boundaries being well defined (Figs 3a and 3b): white-greyish grains (the lightest), a greyish matrix and dark

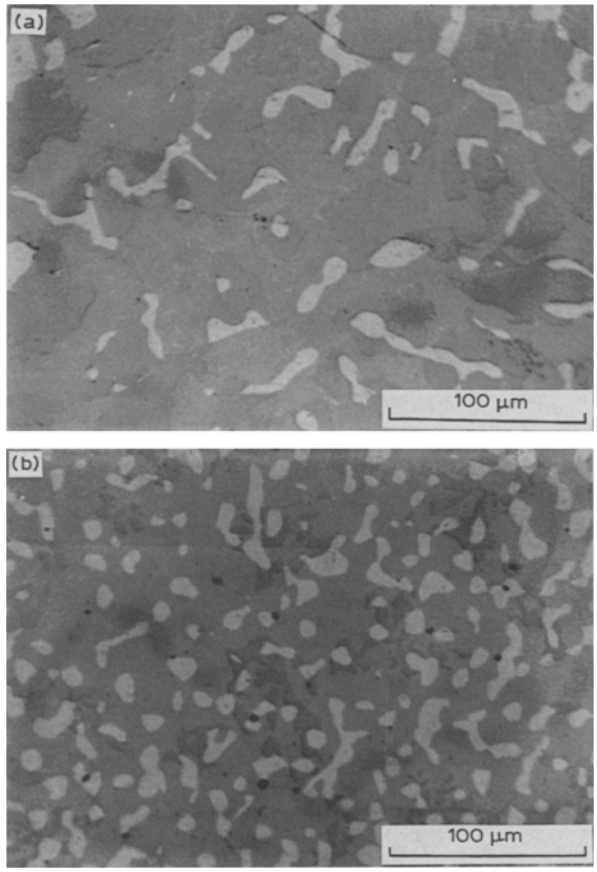

Fig. 3. Annealed Cu–Al–Ag alloys after mechanical polishing: (a) alloy B; (b) alloy C.

grains. In alloy A this is not observable because it was only extruded, not annealed, and therefore a non-equilibrium structure is expected.

According to Adorno's X-ray diffraction and EDS studies [6, 7], these annealed copper based Cu–Al–Ag alloys are composed of three distinct phases: a solid solution of aluminium and silver in the copper (phase α_1); a solid solution of aluminium and copper in the silver (phase α_2, having approximately composition 93% Ag–5.5% Cu–1.5% Al) and a compound having the composition Al_4Cu_9 (phase γ).

Figures 4a and 4b show the micrographs of the alloy C after etching in solutions R_1 and R_2, respectively. Because of the highly oxidizing nature of the reagent R_1, all the surface is attacked. As is usual when employing such a reagent, the darker areas on the micrograph 4a can be attributed to the silver enriched regions and the lighter areas to the copper enriched zones. Alloy B behaves similarly to alloy C. When using such a reagent with alloy A, only a fine dispersion of the dark areas, that is the silver enriched regions, is observed. When the surfaces of the polished alloys are etched by solution R_2 for a very short period (Fig. 4b), approximately one second, the regions rich in silver are not attacked and appear equal to the lightest zones of the only polished specimens (*cf.* Figs 3a and 3b). The dark stains shown in Fig. 4b correspond to the darker areas of Fig. 3b.

Backscattered electron images (BEI) of the alloys after mechanical polishing are shown in Figs 5a–c. In such figures, the lightest areas correspond to the

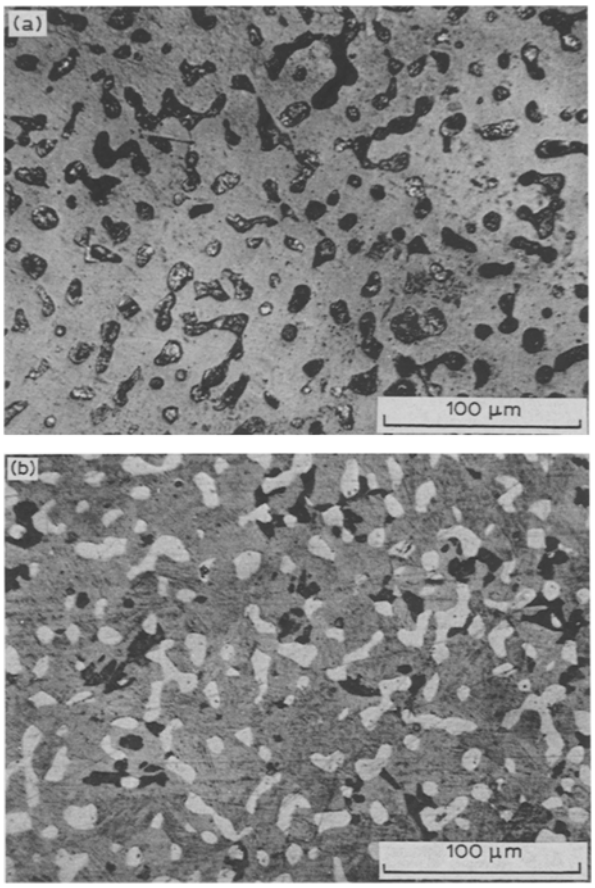

Fig. 4. Alloy C after etching the mechanically polished specimens in (a) reagent R_1 and (b) reagent R_2.

element with higher atomic weight, silver in this case. Fig. 5a shows a fine dispersion of silver enriched segregates when compared with alloys B and C (Figs 5b and 5c, respectively). In alloys B and C, the same three different regions noted by simple metallographic examination can be observed (*cf.* Figs 3a and 3b). The darker areas in Figs 5b and 5c correspond to those zones enriched in the element with lower atomic weight, that is aluminium in our case. X-ray mappings of silver and copper for the alloy C, which are shown in Figs 6a and 6b, confirm the low concentration of silver in the copper enriched zones and the low concentration of copper in those which are silver enriched. Accordingly, the white-greyish regions appearing in the micrographs 3a (alloy B) and 3b (alloy C) correspond to the phase α_2, the greyish matrix to the phase α_1 and the darker grains to the phase γ. Semiquantitative analysis by EDS of the darker grains show the existence of 95% of Cu, about 4% of aluminium and a small amount of silver (less than 1%). This indicates that in the darker grains, the phase γ coexists with a small quantity of phase α_1. Alloy C shows a higher quantity of phase α_2 than alloy B, as expected, since the former has a higher silver content.

The secondary electron images (SEI) of the alloy surface show that the surface morphology of the alloys is considerably altered after the RTPS (cf. Figs 7a, 8a and 9a). On the other hand, the microanalysis performed by EDS clearly demonstrates that aluminium is not present on the electrode surface in these con-

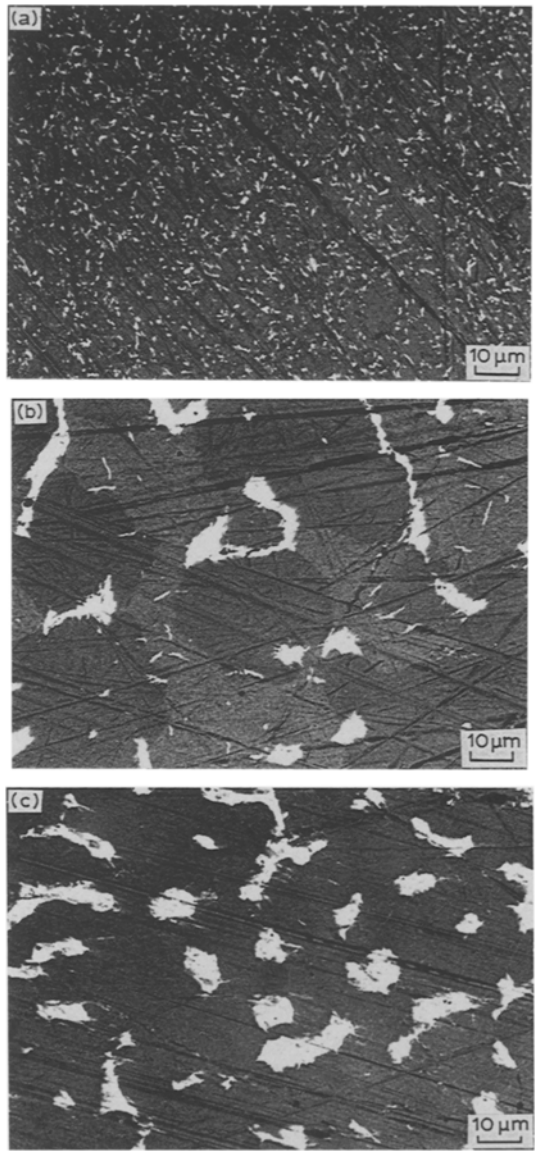

Fig. 5. SEM backscattering micrographs of Cu–Al–Ag alloys after mechanical polishing: (a) alloy A; (b) alloy B and (c) alloy C.

ditions (see the experimental details). Chemical analysis of the electrolyte after the RTPS of the alloy A gave the following concentrations of the cations in solution: $[Cu^{2+}] = 230\,ng\,cm^{-3}$; $[Ag^{+}] < 50\,ng\,cm^{-3}$ and $[Al^{3+}] = 800\,ng\,cm^{-3}$. These results clearly indicate a preferential dissolution of aluminium and the low solubility of copper and silver in the working electrolyte. The ratio between the anodic and cathodic charges in the quasistationary cyclic polarizations is approximately unity. Therefore, the change in the morphology of the surface is basically due to the surface roughening resulting from successive oxidations and reductions, in which the electrodeposits formed in the anodic sweep are reduced with high efficiency in the cathodic sweep.

The SEI and BEI in Figs 8a and 8b show interesting aspects of the surface structure of the alloy B after the RTPS. The silver enriched grains, the lightest in Fig. 8b, already exhibit ridges of the mechanical polishing, in agreement with the small charge employed in the oxidation-reduction cycles of silver (*cf.* Fig. 2b). The copper matrix has a high roughness as a conse-

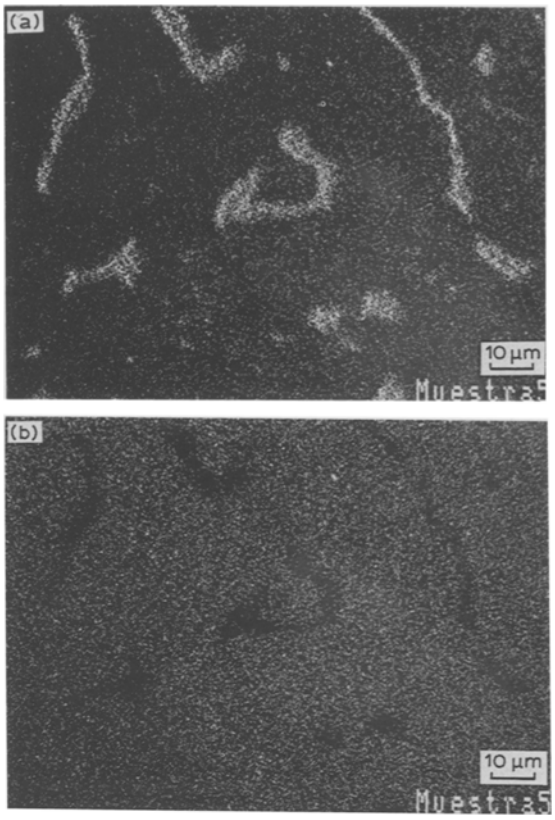

Fig. 6. X-ray mapping of the elements of alloy B, corresponding to Fig. 5b: (a) mapping of Ag and (b) mapping of copper.

quence of the quantity of charge employed in the surface reformation (*cf.* Figs 8a and 2b). The two round grains on the left of Figs 8a and 8b are grains of the phase which have lost their aluminium. As shown by EDS, these round grains contain a certain quantity of silver, probably as a result of silver species

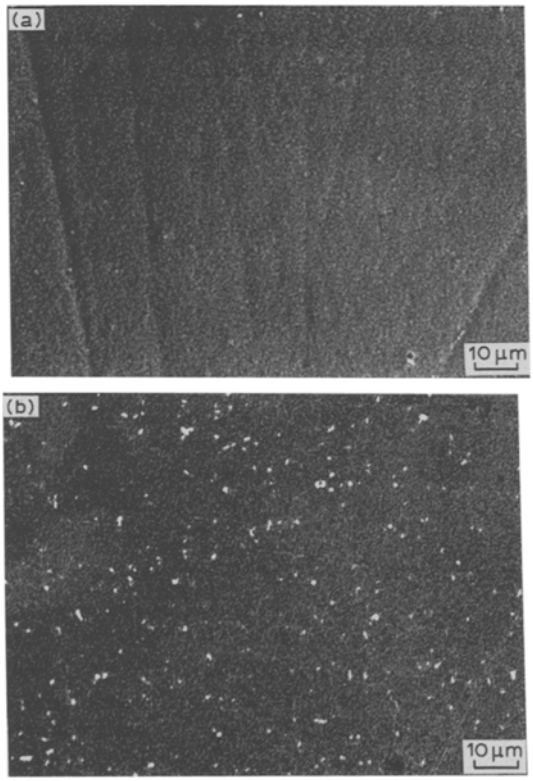

Fig. 7. Structure of the alloy A after 1 h of RTPS at $100\,mV\,s^{-1}$: (a) SEI and (b) BEI.

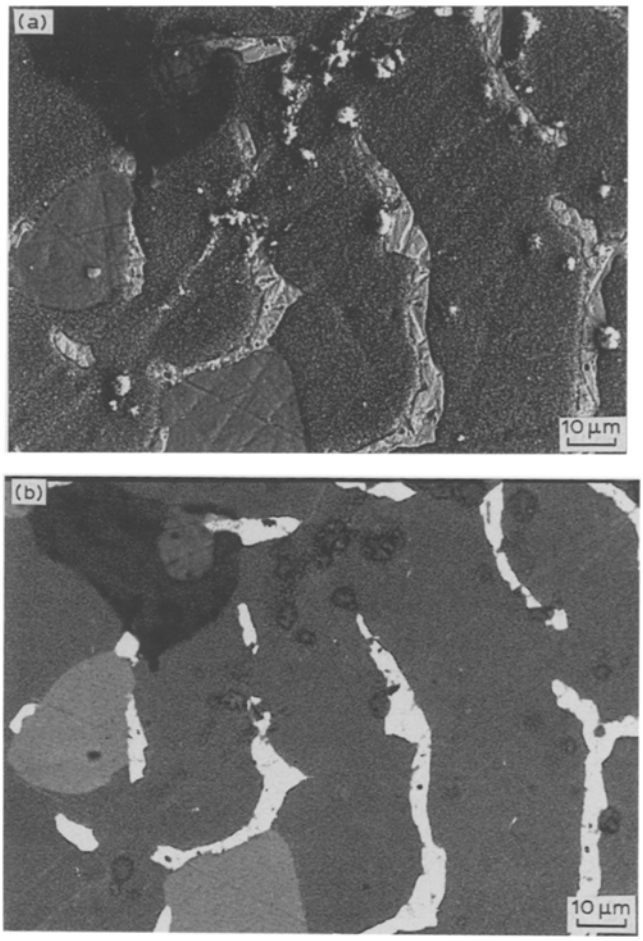

Fig. 8. Structure of the alloy B after 1 h of RTPS at $100\,mV\,s^{-1}$: (a) SEI and (b) BEI.

reduction on copper. The ridges and the low roughness of these round grains when compared with the copper matrix clearly show that the latter is a more electroactive zone. In alloy C, round grains with characteristics similar to those described for alloy B have not been found. This may be due to the much lower γ phase content of alloy C.

Two more phases can be observed in the micrographs 8a and 8b: the dark zone shown in the upper part of Fig. 8a and the small prominent precipitates distributed on the alloy surface. Both phases show only the copper signal by EDS. As long as the darker areas in Fig. 8b correspond to a mean atomic weight lower than that of the copper matrix, both phases are attributable to residues of copper oxide not reduced in the cathodic sweep.

There are also evidences of the copper deposition on silver enriched grains, since in Fig. 7b less silver enriched areas than in Fig. 5a, corresponding to the mechanically polished alloy, can be seen on the surface. Moreover, in Fig. 8a, copper oxide appears covering certain parts of the silver enriched grains.

From these results, it is suggested that the following sequence of events takes place during the first cyclic polarization of alloy B: (1) In the anodic sweep, Al is preferentially dissolved from phase γ while Cu forms an oxide basically on phase α_1; copper oxide spreads on phase α_2 (silver is not yet oxidized). (2) Silver forms

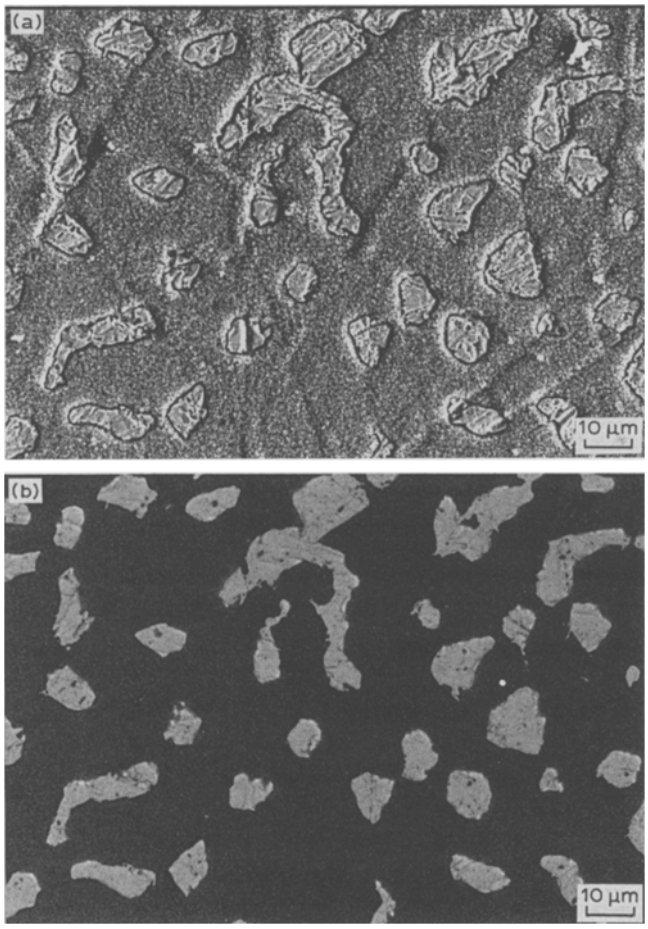

Fig. 9. Structure of the alloy C after 1 h of RTPS at $100\,mV\,s^{-1}$: (a) SEI and (b) BEI.

silver oxides on phase α_2; such an oxide spreads on phase γ, which show small content of copper oxides (because of preferential dissolution of aluminium). (3) In the cathodic sweep, silver oxide is the first to be reduced to silver and, therefore, silver is deposited on phase α_2 and on those regions of phase γ previously covered by silver oxide. (4) Finally, copper oxides are reduced to copper on phases α_1, γ and on the zones of phase α_2 previously covered by copper oxides. In the next consecutive cycles, the same sequence of events takes place, the following having increasing importance: (a) aluminium elimination from the surface of the alloy; (b) silver spreading on phase γ as an electrodeposit which protects the copper in phase γ from further oxidation so that grains of phase γ are less attacked than those of phase α_1 (copper is oxidized before silver); (c) copper spreading on phase α_2 and (d) as long as copper species are oxidized and reduced at potentials basically different from those of silver, the RTPS leads to a surface dealloying and the response of the electrode is the superposition of the quasistationary cyclic polarizations of high purity copper and silver.

The same scheme can be used to interpret the surface reformation when using the alloys A and C. However, there are minor differences because alloy A does not have the phase γ and the alloy C contains only a small quantity of such a phase. In alloy C, the grains of the γ phase are too small and, they are not observed after the RTPS.

3. Conclusions

It is concluded that consecutive cyclic polarization when using Cu–Al–Ag alloys in 0.5 M NaOH leads to aluminium elimination from the surface and to an important surface reformation. Such a surface reformation consists of a roughness increase because of the cyclic oxidation-reduction processes in which the ratio of anodic to cathodic charge is near unity. Copper and silver oxidized species have low solubility in this medium. There is evidence of copper deposition on silver and also of silver on copper because of the spread of the corresponding oxides. The quasistationary cyclic polarization curves consist in the superposition of the quasistationary cyclic polarization curves of high-purity copper and silver because of the surface dealloying. Further studies on the electrochemical behaviour of Cu–Al–Ag alloys which have been submitted to a RTPS treatment in alkaline solutions must take into account such a surface reformation.

Acknowledgements

Financial support from the *Consejo Superior de Investigaciones Científicas* (CSIC), Spain, and the *Conselho Nacional de Desenvolvimento Científico e Tecnológico* (CNPq), Brazil, are gratefully acknowledged. The authors wish to thank the *Servei Científico-Tècnic de la Universitat de Barcelona* for the provision of laboratory facilities and Dr R. Fontarnau, Dr A. T. Adorno and Dr W. Garlipp for useful discussions.

References

[1] C. Panseri and M. Leoni, *Alluminio* **30** (1961) 289.
[2] R. Z. Nakazato, A. C. Guastaldi, A. V. Benedetti and M. Cilense, Proceedings of the 12th SENACOR conference, Brazil (1985) p. 62.
[3] T. B. Massalski and J. H. Perepezko, *Z. Metallkde.* **64** (1973) 176.
[4] A. T. Adorno, M. Cilense and W. Garlipp, *J. Mater. Sci. Lett.* **6** (1987) 163.
[5] A. V. Benedetti, M. Cilense, A. C. Guastaldi, R. Z. Nakazato and E. Tengnon, results not yet published.
[6] A. T. Adorno, M. Cilense and W. Garlipp, *J. Mater. Sci. Lett.* **8** (1989) 281.
[7] A. T. Adorno, PhD Thesis, Univ. of São Paulo, São Carlos, Brazil (1987) p. 135.
[8] R. Z. Nakazato, P. T. A. Sumodjo and A. V. Benedetti, *Portugaliae Electrochim. Acta* **5** (1987) 263.